Supplementary Materials and Methods

Generation of *kumo*$^{M41-13}$ allele

kumo^{M41-13} allele was generated by deleting the first exon containing the possible start codon. To generate this allele a region between two piggyback insertions in CG14306, which codes for RING and B-box domains present at N-terminus of Kumo, was deleted. The two piggyback insertions *PBacCG14306[e01936]* and *PBac{WH}CG14306[f05204]*, located 460 nucleotides apart in CG14306 were selected. A FLP mediated recombination was used to remove the region between the two piggyback insertions (Thibault et al, 2004).

Drosophila strains *y w* and *kumo*$^{M41-13}$*/TM3* were used as control. Following alleles were used, *mnk*^{p6}, *meiW68*^{1}, and *mei41*^{D3}.

Generation of *kumo* transgenic flies

Transgenic flies harbouring full length, N-terminal (containing RING and B-box domains) and C-terminal (containing all five tudor domains) of Kumo, were generated. The regions of Full-length Kumo, Kumo-CT and Kumo-NT were amplified using the primer sets; Kumo-cds-Fw & CG14303-10-Rv, Kumo-cds-Fw & KumoNT-Rv, and KumoCT-Fw & CG14303-Rv, respectively. Amplified fragments were cloned into pENTR™/D-TOPO (Invitrogen), and then recombined into pPMW (The Drosophila Gateway Vector Collection) following manufacturer's instructions. All primers are listed in Supplementary Table S2. Plasmids were injected into *y w* embryos to generate transgenic flies using the standard protocol. The expression of transgenes was driven in germline by *NGT40*; *nosGal4-Vp16* driver.

Antibodies

The antibodies used for immunostaining were as follows. Rabbit anti-Otefin (1:100) (a kind gift from Dr. Dahua Chen), guinea pig anti-Rhino (1:1000, kindly provided by Dr. William Theurkauf), mouse monoclonal anti-HP1 (C1A9, Developmental Studies, 1:50), rabbit anti-H3K9Me2 and anti-H3K9Me3 (1:200, Upstate, 07-441, 07-442, respectively).

Antibody Generation

Rabbit anti-Kumo, antisera were generated against a portion of GST-tagged Kumo (aa 1503 to aa1593). Peptides were purified according to the manufacture's protocol and injected into animals with complete or incomplete adjuvant (Thermo Scientific/ Pierce).

In vitro IP Experiments

Interaction of Kumo with other nuage components were examined in S2 cells with Kumo-FL, Kumo-CT and Kumo-NT cloned in pENTR™/D-TOPO, using primer sets Kumo1stATG-Fw, CG14303-10 Rv, Kumo1stATG-Fw, KumoNT-Rv and KumoCT-Fw and CG14303-10Rv, respectively (sequences in Table S2). Those entry vectors were recombined with pAFW, or pAMW (The Drosophila Gateway Vector Collection) in accordance with manufacturer's protocol. SpnE and Aub cloned in pAMW were generated as described by Patil and Kai 2010. S2 cells were transfected using cellfectin (Invitrogen), and Co-IP experiments were performed after 48 hrs of transfection as previously described (Patil & Kai, 2010). Briefly, the cells after 48 hours of transfection were lysed in IP buffer, and lysate was incubated in equilibrated protein A/G beads (Calbiochem) before incubation with antibody-conjugated beads overnight. After washing the beads three times in IP buffer, proteins were eluted at 95^0C SDS loading buffer. Western blotting was performed using standard procedure.

Strand specific RT-PCR

The total RNA was prepared from whole ovaries using TriZol method. First strand cDNA synthesis was performed with plus or minus strand primers spiked with rp49-Rv primer for control. RNA levels from cluster 1A and cluster 1-32 were assessed as described by Klattenhoff et al., 2009 (represented as 42AB1 and 42AB2, Fig. 7A, Table S2), in addition to two more regions near cluster 1A (42AB3 and 42AB4). Primers for 1A and cluster 1-32 were renamed as 42AB1-plusRT, 42AB1minus-RT & 42AB2-plusRT, 42AB2-minusRT Table S2). In addition precursor transcripts (region near to cluster 1A) from plus and minus stands were reverse transcribed using 42AB3-plus 42AB3-minus and 42AB4-plus and 42AB4-minus. First strand cDNA synthesis was performed using SuperScriptIII^{TM} reverse transcriptase (Invitrogen, 18080-093), following the manufacturer's instructions. The resulting cDNAs for plus and minus strands were subjected to quantitative real-time PCR using the primers indicated for each cluster (Supplemental Table S2). qPCR reactions were performed using a SYBR Green (Invitrogen, 11780-200) in ABI 7900 HT Fast Real-time

PCR system (Applied Biosystems). The expression level of strand specific RNA was measured relative to the *rp49* internal control. No reverse transcriptase control reactions did not yield any significant signal. Three biological replicates were performed, and each time three technical replicates were performed for each RT primer. Standard errors were calculated for three biological replicates.

Quantitative RT-PCR

Expression levels of transposons (see table S2 for primers) were monitored in *kumo* mutants and control ovaries by quantitative RT-PCR. cDNA was prepared with 2 µg of total RNA using SuperscriptIII reverse transcriptase (Invitrogen). qRT-PCR reactions were performed using SYBR mix (Invitrogen) in ABI7900 HT Fast Real-time PCR system (Applied Biosystems). The expression levels were normalized by housekeeping controls, *Actin-5c* and *rp49*, followed by comparison of expression levels between mutant and controls.

Small RNA sequencing and analysis

Small RNA ranging from 20-30 nucleotides in size, from *kumo* mutant and heterozygous ovaries, were extracted from gel and were subjected to library preparation for sequencing using Illumina GAIIX platform (done with help of Macrogen Inc., Seoul). FASTX files for each library was trimmed for adapter, and sequences having low quality scores were discarded before analysis, using Galaxy toolbox (http://main.g2.bx.psu.edu/). Small RNA reads after filtering above were used for downstream analysis. Drosophila genome Release 5.25 was used as reference, canonical transposon sequences were obtained from flybase (http://www.fruitfly.org/p_disrupt/TE.html), non-coding RNAs were obtained from rfam, (http://rfam.sanger.ac.uk) piRNA cluster information was taken from Brennecke et al, 2007. Trimmed sequences were aligned to the above mentioned databases using Bowtie (Langmead et al, 2009), and the library sequences were aligned to genome to analyze alignment to piRNA clusters (Brennecke et al, 2007). Data of the two libraries, the heterozygous and the mutant, were normalized to the non-coding RNA and endo-siRNAs, which are derived from two major hairpins (Okamura et al, 2008). Alignments were stored, examined and compared using Samtools (Li et al, 2009), BEDTools (Quinlan & Hall, 2010) and UCSC genome browser utilities (http://genome.ucsc.edu/). Sequences mapping to the plus strand and minus strands were plotted on the top and bottom on the cluster profiles. All the reads were aligned to canonical transposon. Small RNAs matching to the sense and antisense strands were counted and density plots were made as described above.

Brennecke J, Aravin AA, Stark A, Dus M, Kellis M, Sachidanandam R, Hannon GJ (2007) Discrete small RNA-generating loci as master regulators of transposon activity in Drosophila. *Cell* **128:** 1089-1103

Langmead B, Trapnell C, Pop M, Salzberg SL (2009) Ultrafast and memory-efficient alignment of short DNA sequences to the human genome. *Genome Biol* **10:** R25

Li H, Handsaker B, Wysoker A, Fennell T, Ruan J, Homer N, Marth G, Abecasis G, Durbin R (2009) The Sequence Alignment/Map format and SAMtools. *Bioinformatics* **25:** 2078-2079

Okamura K, Chung WJ, Ruby JG, Guo H, Bartel DP, Lai EC (2008) The Drosophila hairpin RNA pathway generates endogenous short interfering RNAs. *Nature* **453:** 803-806

Patil VS, Kai T (2010) Repression of Retroelements in Drosophila Germline via piRNA Pathway by the Tudor Domain Protein Tejas. *Curr Biol*

Quinlan AR, Hall IM (2010) BEDTools: a flexible suite of utilities for comparing genomic features. *Bioinformatics* **26:** 841-842

Thibault ST, Singer MA, Miyazaki WY, Milash B, Dompe NA, Singh CM, Buchholz R, Demsky M, Fawcett R, Francis-Lang HL, Ryner L, Cheung LM, Chong A, Erickson C, Fisher WW, Greer K, Hartouni SR, Howie E, Jakkula L, Joo D, Killpack K, Laufer A, Mazzotta J, Smith RD, Stevens LM, Stuber C, Tan LR, Ventura R, Woo A, Zakrajsek I, Zhao L, Chen F, Swimmer C, Kopczynski C, Duyk G, Winberg ML, Margolis J (2004) A complementary transposon tool kit for Drosophila melanogaster using P and piggyBac. *Nat Genet* **36:** 283-287

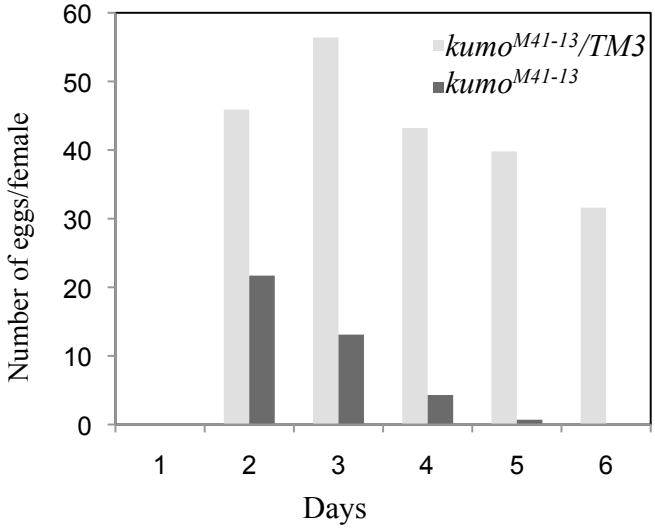

Figure S1. *kumo* mutant flies lay fewer number of eggs. Comparison of egg laying between *kumo*$^{M41\text{-}13}$*/TM3 and kumo*$^{M41\text{-}13}$ flies from day one to six after hatching.

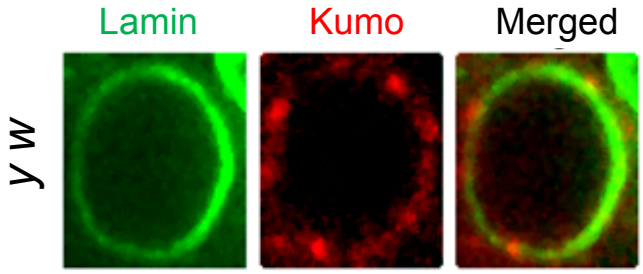

Figure S2. Kumo localizes to cytoplasmic face of the nuclear envelop. A nurse cell nucleus stained for Lamin (Green) and Kumo (red). Perinuclear localization of Kumo is discernible.

A

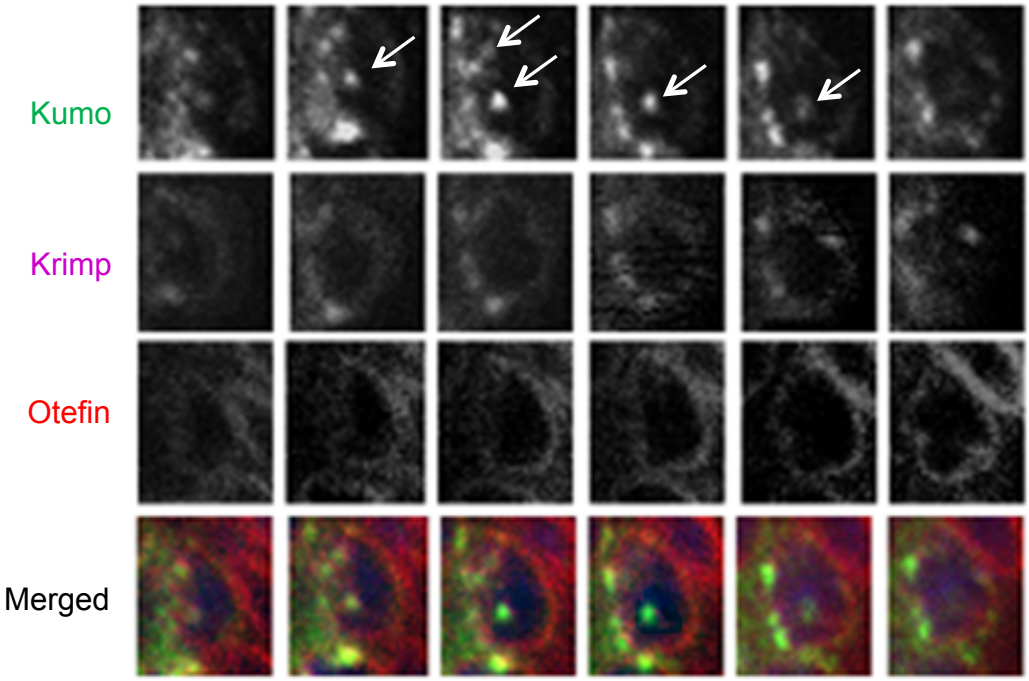

Figure S3. Myc-Kumo localizes to nucleus in addition to perinuclear nuage, not Krimper another nuage component. (A) Optical sections of a germline cells in germarium showing Myc-Kumo (green) localization to perinuclear region and to nucleus (indicated by arrows), localization for Krimp (Magenta) was observed mostly to perinuclear region. Nuclear membrane was stained for Otefin (red).

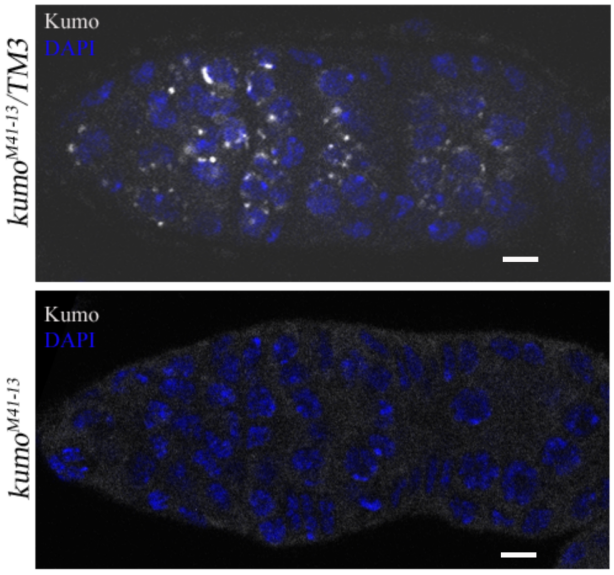

Figure S4. Loss of Kumo localization signal in kumo mutants. Immunostaining with anti-Kumo antibody shows absence of signal of Kumo localization (white) in *kumo* mutants. Nuclei were counterstained with DAPI. Scale bar: 5μm.

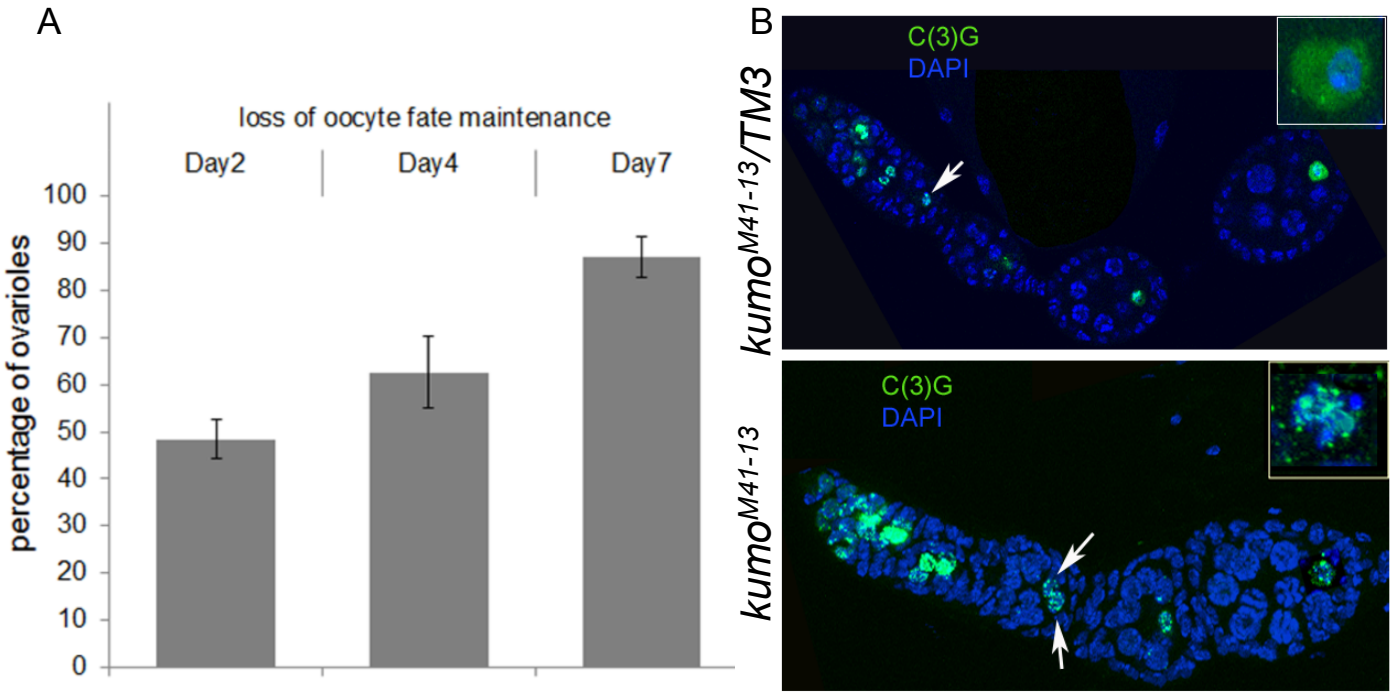

Figure S5. Delay in oocyte fate maintenance, karyosome compaction and defect in polarity establishment in *kumo* mutants. (A) Loss of oocyte fate maintenance in *kumo* mutants; number of *kumo* mutant ovarioles that show loss of oocyte by Orb staining were calculated, on the days 2 (n=146), 4 (n=83) and 6 (n=109). (B) Delay of oocyte fate determination and failure of karyosome compaction in *kumo* mutants; C(3)G staining (green) shows a single oocyte in region 3 of germarium, indicated by arrow, and karyosome compaction (inset) in a stage 3 egg chamber, in *kumo* heterozygous ovaries. However, *kumo* mutants show at least two C(3)G positive nuclei in region 3 and stage 1 egg chamber, indicated by arrows, and C(3)G in oocyte nuclear in stage 4 egg chamber (inset). Nuclei were stained by DAPI.

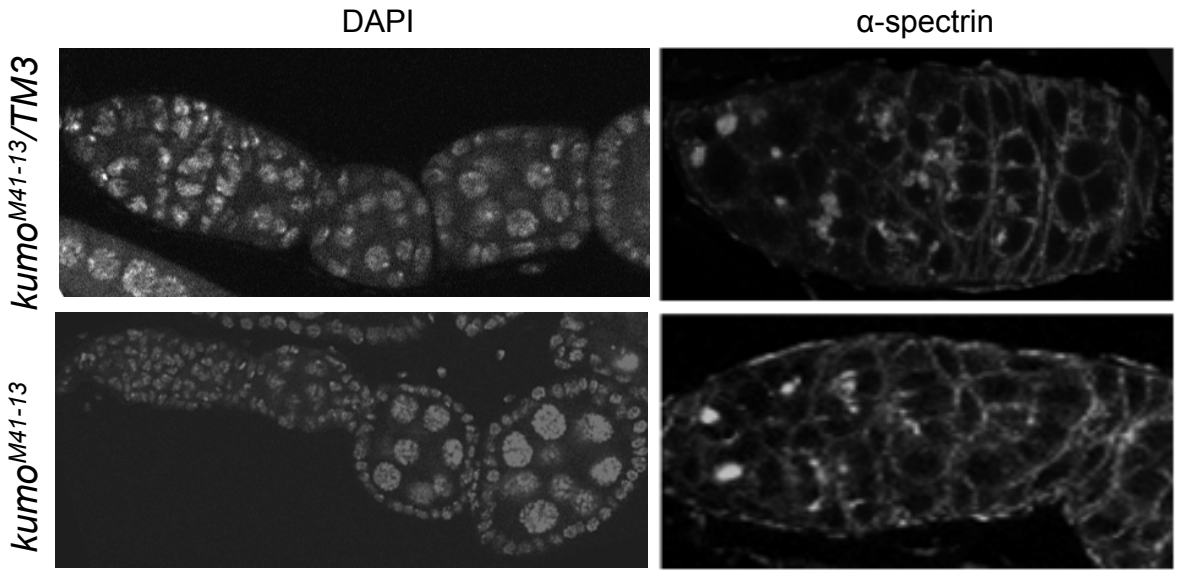

Figure S6. Germline stem cells are present in the 15 days-old *kumo* mutant ovarioles. Ovarioles and germaria from 15-days old flies were stained with DAPI and anti-α-spectrin are shown. Early stages of egg chambers and germarium containing germline cells with round fusome and branched fusome in 15 days old *kumo* mutant females, indicating the presence of GSCs and no significant defects in early differentiation.

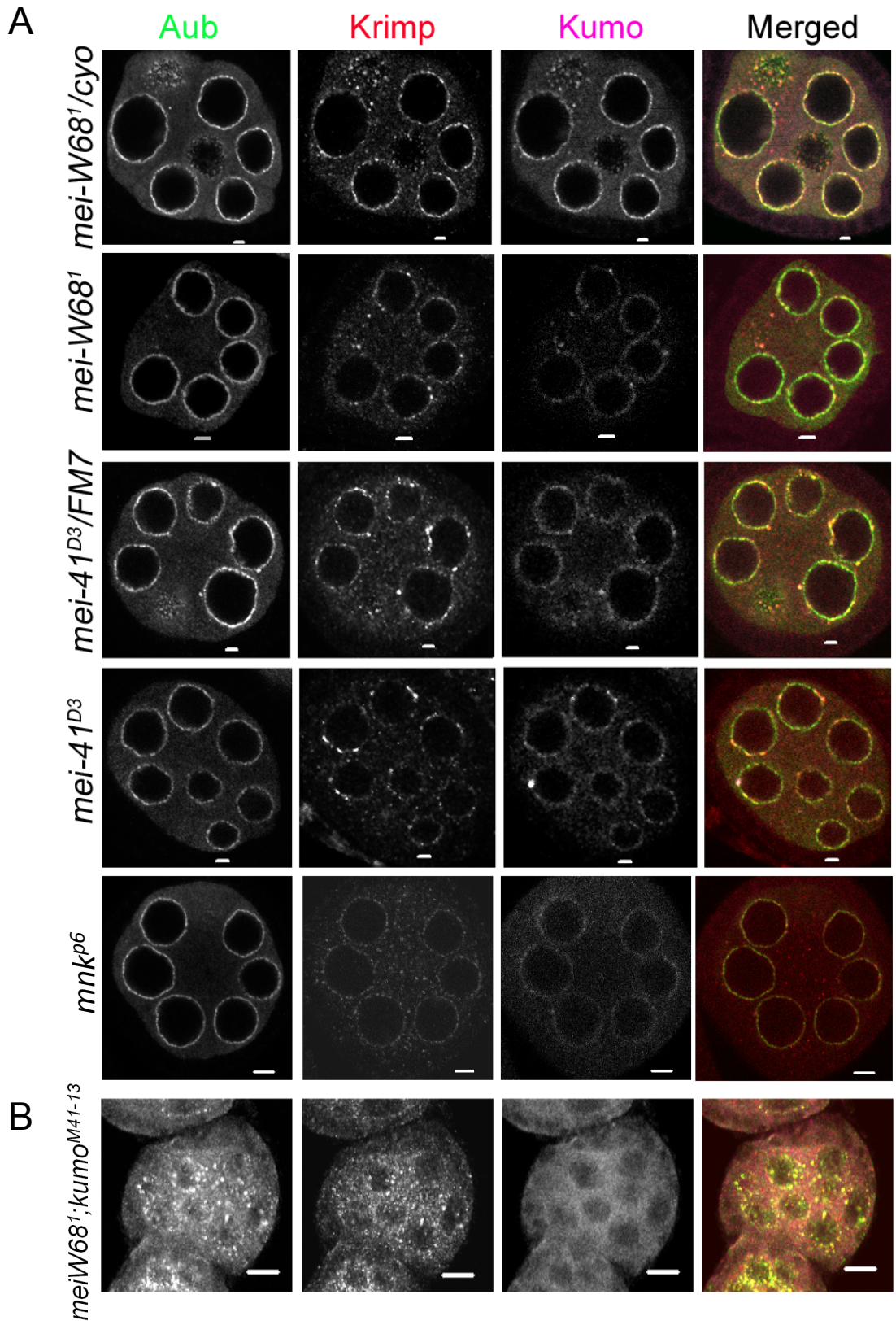

Figure S7. Nuage organization is not affected in the mutants of canonical DNA damage signaling pathway. (A) Immunolocalization of Aub (Green), Krimp (red) and Kumo (magenta) in the *meiW68* and *mei41* heterozygous and mutant ovaries shows nuage is not affected in absence of DNA damage signaling pathway. (B) Aub (green) and Krimp (red) remain mislocalized from their characteristic perinuclear position in *meiW68* and *kumo* double mutant, indicating DNA damage pathway mutation does not rescue nuage localization in the *kumo* mutants.

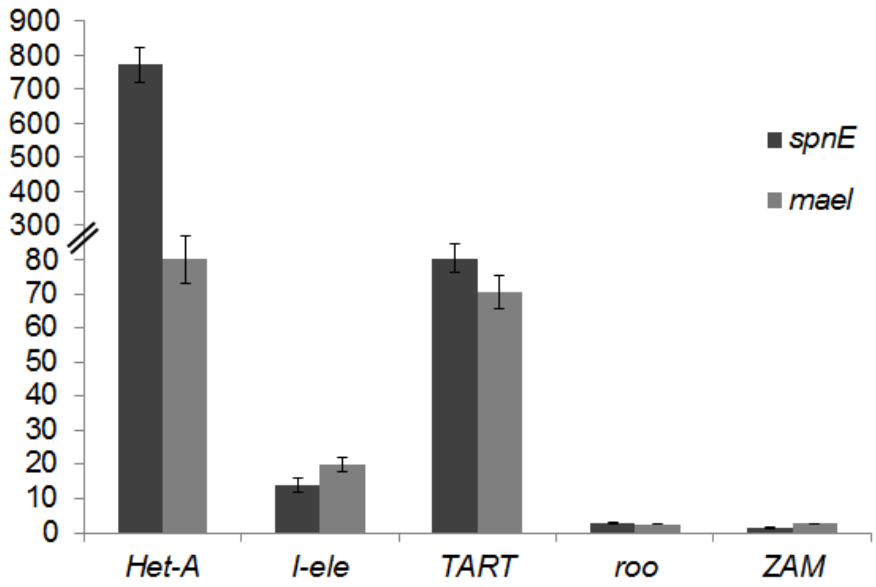

Figure S8. Derepression of reteroelements in the *spnE* and the *mael* mutant ovaries. Quantitative RT-PCR showing the fold upregulation of reteroelements in the *spnE* and *mael* mutants ovaries in comparison to respective heterozygous ovaries. Error bars indicate standard error for quadruple PCR replicates.

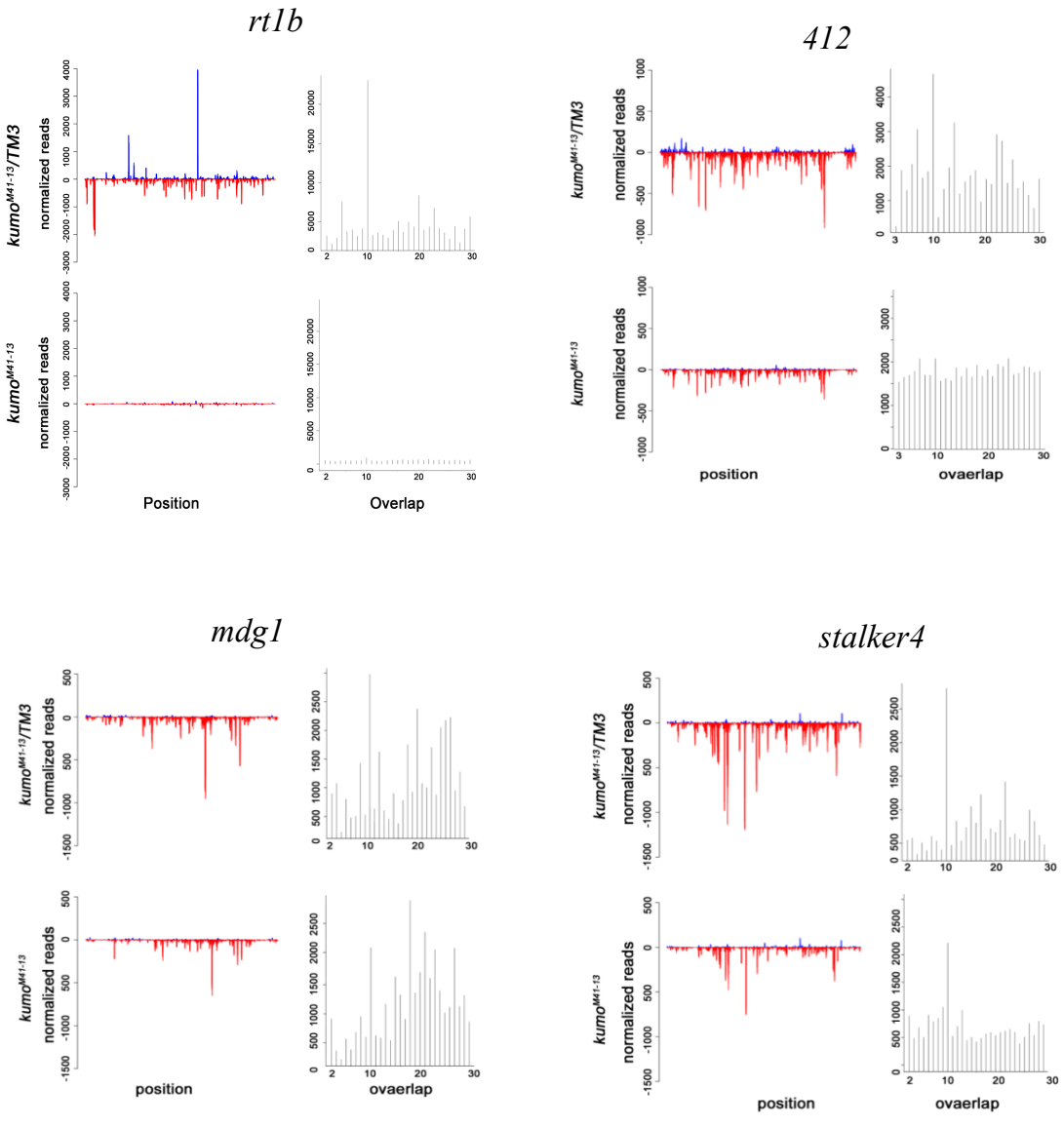

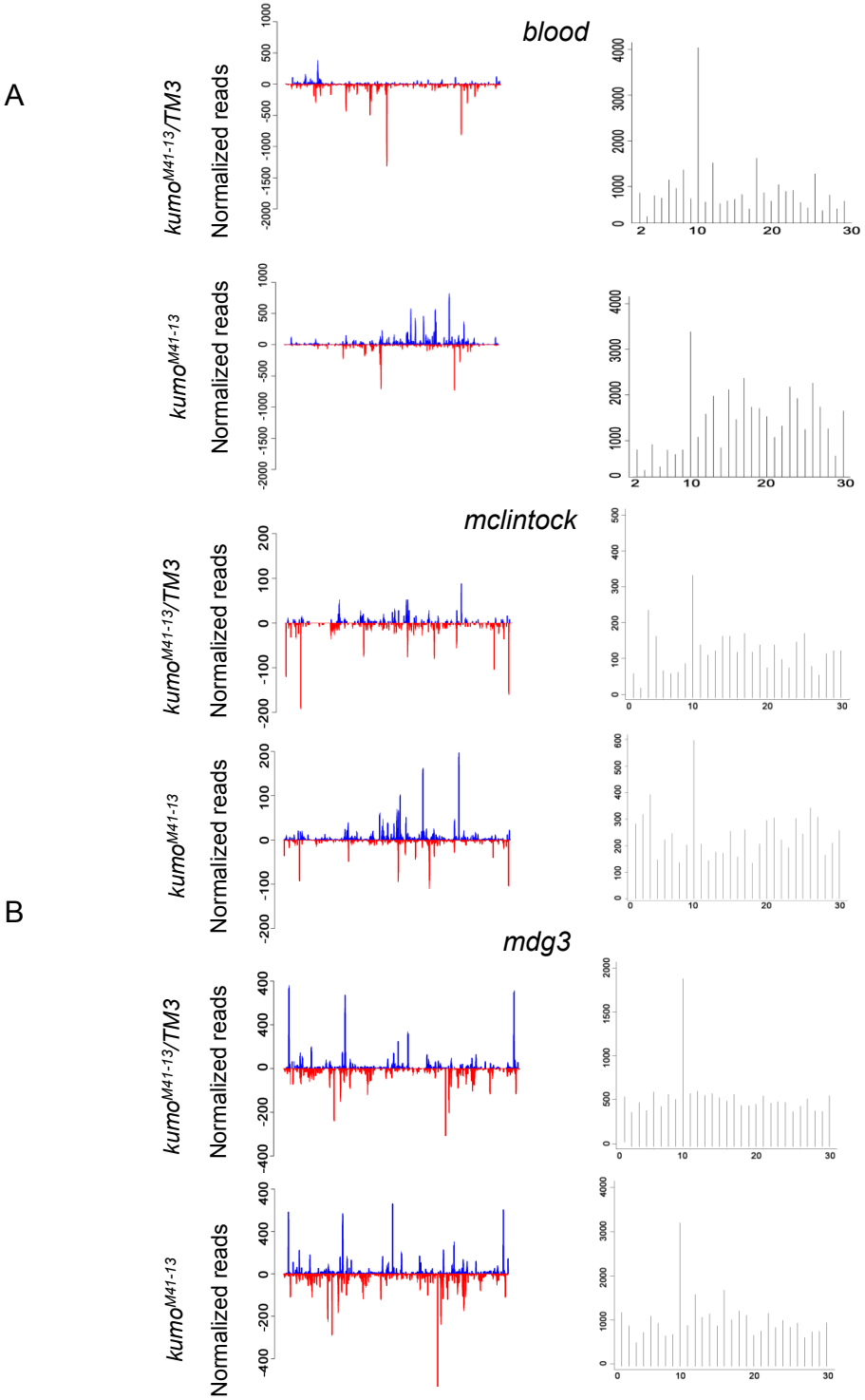

Figure S9. Analysis of piRNAs for transposons. Analysis of piRNA mapping to transposons having predominant germline expression (*rt1b*) and both germline and somatic expression (*blood*, *412*, *mdg1*, *mdg3*, *stalker4* and *mclintock*). Left panels: piRNAs mapped to consensus sequence on sense (blue) and antisense (red) strands. Right panels: piRNA showing 10 nt overlap. A severe reduction in sense and antisense piRNA, and piRNAs that overlap by 10 nt for *Rt1b* are observed in the *kumo* mutants. A mild reduction in antisense piRNAs matching to *412, mdg1,* and *stalker4 was* observed in the *kumo* mutant. piRNAs showing 10nt overlap were reduced for *412* and *mdg1*, while no significant reduction in those was observed for *stalker4* and *blood.* piRNA mapping to sense strand were increase for *blood, mclintock* and *mdg3.*

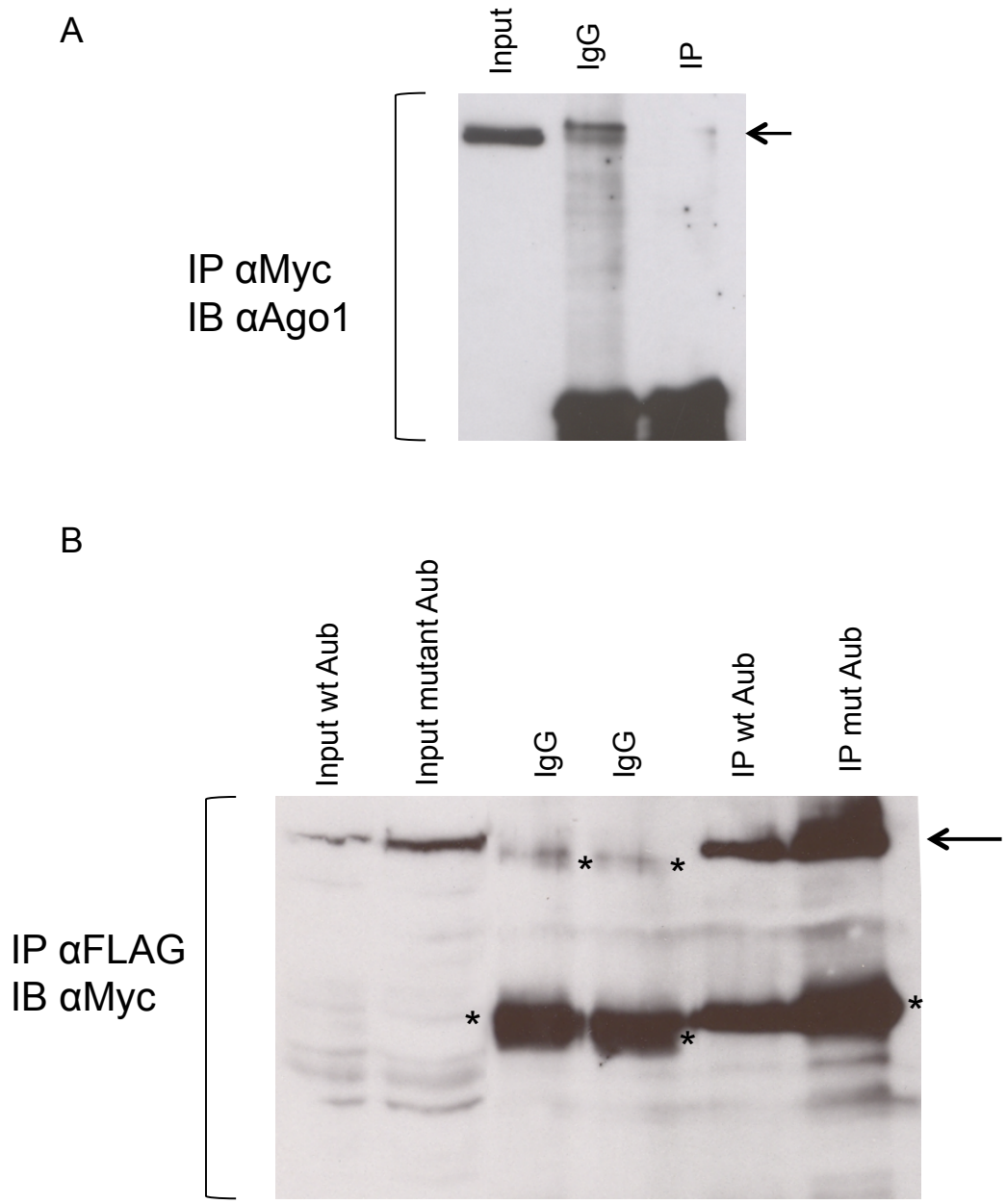

Figure S10. Kumo does not interact with Ago1, and interacts with Aub in a sDMA-independent manner

(A)Immunoprecipitation with anti-Myc antibodies was performed using ovarian lysates expressing Myc-Kumo. Ago1 was not co-precipitated with Myc-Kumo.

(B) FLAG-Kumo was co-transfected either with the wild-type or the mutated Myc-tagged Aub. Kumo co-precipitates with both wild-type and the mutated Aub. Asterisks denote non-specific bands.

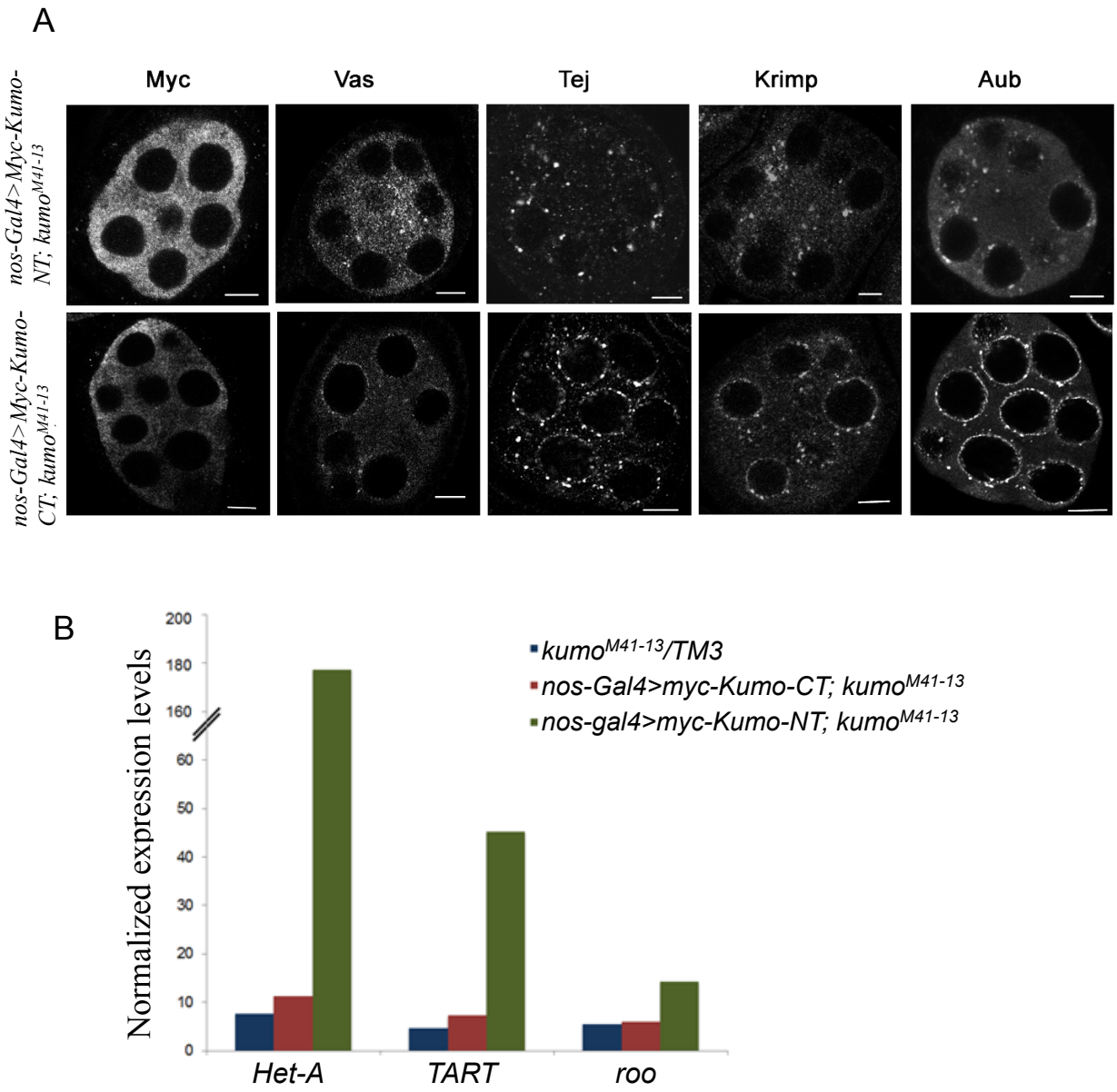

Figure S11. Kumo-CT rescues nuage localization of piRNA pathway components and transposon derepression in *kumo* mutants. (A) Localization of Kumo-CT and Kumo-NT transgenes, driven by nosGal4 in kumo mutants background. Upper panel; localization of Vas, Tej, Krimp and Aub ~~as~~ to dispersed cytoplasmic foci in *kumo* mutant ovaries expressing Kumo-NT. Lower panel; localization of Vas, Tej, Krimp and Aub at the perinuclear nuage and also to some discrete cytoplasmic foci in kumo mutant ovaries expressing Kumo-CT. Scale bars:5µm. (B) Expression levels *of HetA, TART* and *roo* reteroelements in *kumo* heterozygous (blue) and *kumo* ovaries expressing Kumo-NT (green) and Kumo-CT (red) transgenes. Expression levels were compared after normalization with *Actin-5C*. Although Kumo-CT rescues derepression of transposons to large extent, Kumo-NT does not.

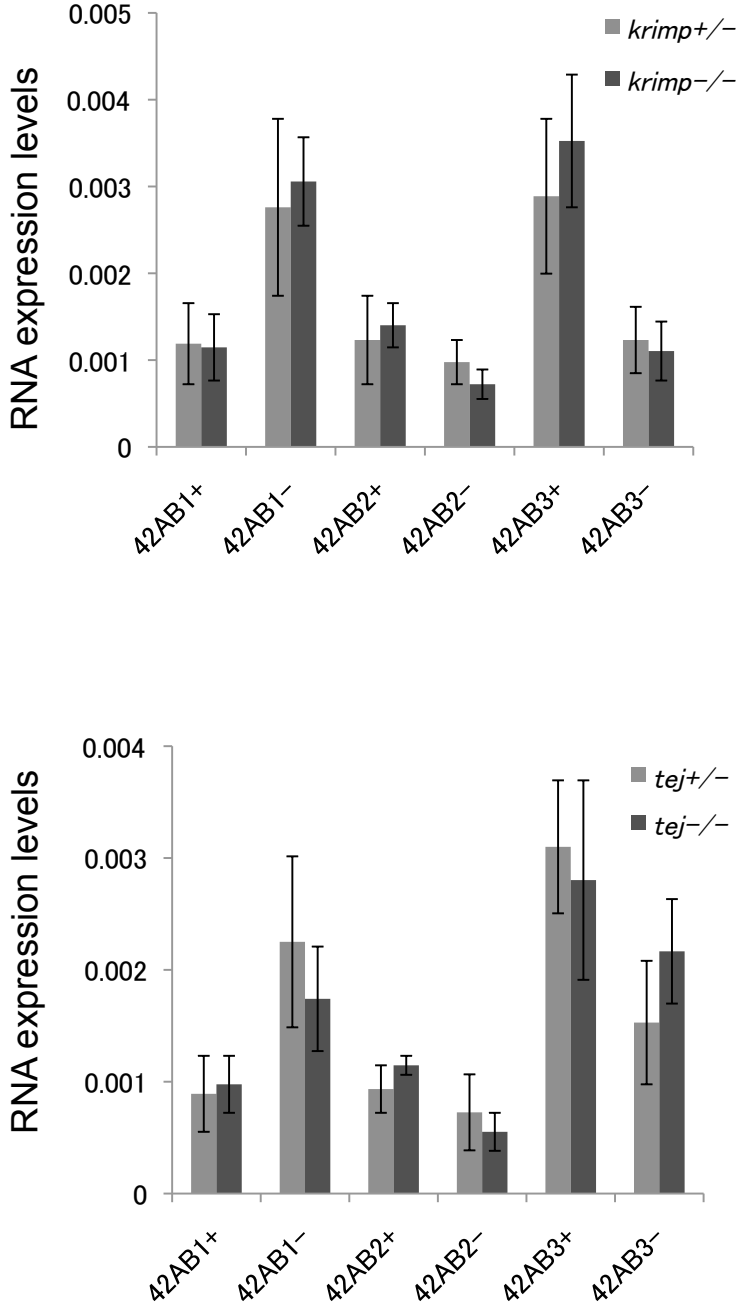

Figure S12. Transcription from cluster *42AB* was not affected in the *tej* and *krimp* mutants. Strand-specific quantitative RT-PCR showing the expression levels of precursor transcripts from the plus and minus strands (indicated by + and -, respectively) from *42AB* piRNA cluster in *tej* and *krimp* mutants ovaries. Expression levels of cluster transcripts from both strands in *tej* and *krimp* mutants do not show and significant difference compared to those in the heterozygous control. Similarly, no significant difference in expression levels of transcripts from a region of *flamenco* piRNA cluster was observed between control and the mutant. Error bars indicate standard error for three independent experiments.

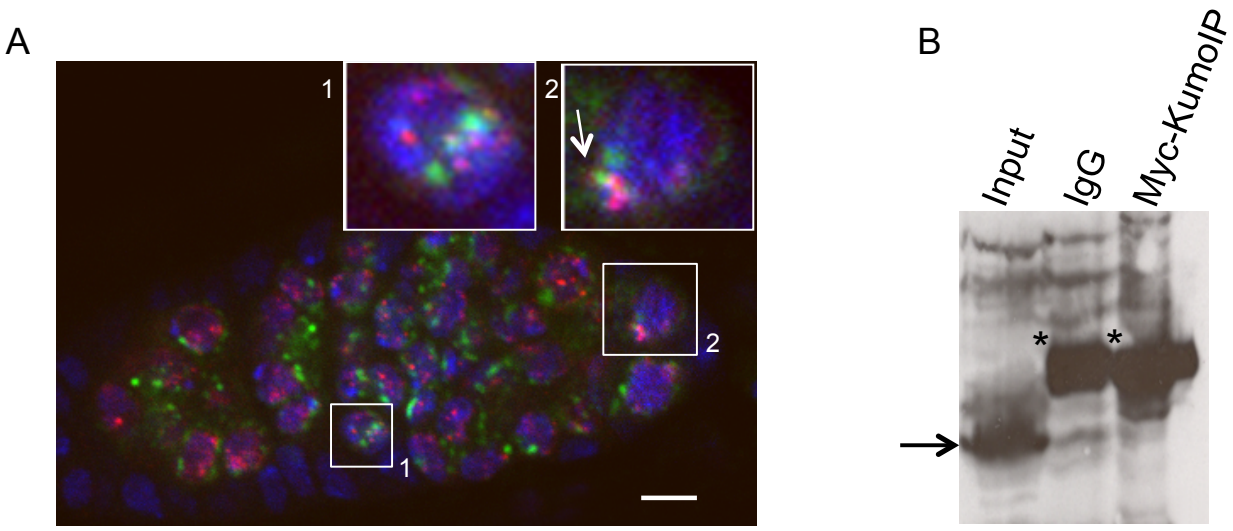

Figure S13. Kumo does not interact with Rhi. (A) Immunostaining for Rhino (red) with Kumo (green) in the germarium, the optical sections shows juxtaposed Rhino and Kumo foci (inset) in some cells. Nuclei were stained with DAPI, scale bar: 5 μM. (B) Myc-Kumo was expressed in germline cells and was immunoprecipitated with anti-Myc antibody. A subsequent western blotting with anti-Rhi antibody indicates Rhi was not be co-precipitated with Myc-Kumo. Asterisks represent non-specific bands.

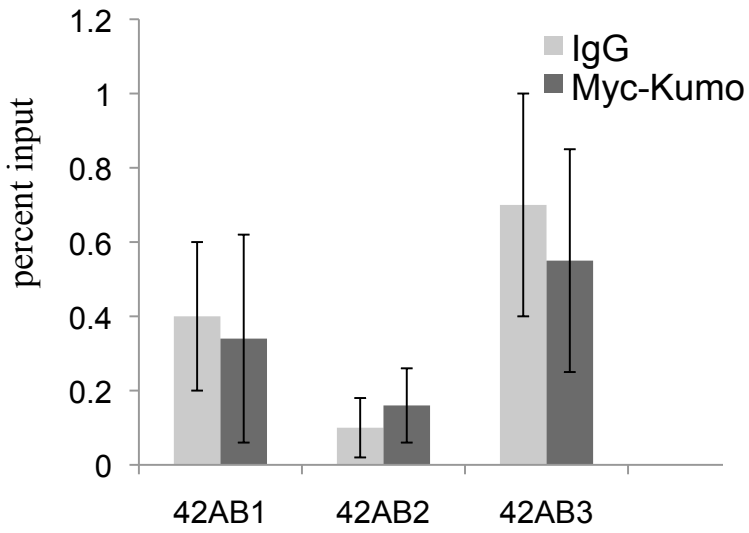

Figure S14. Myc-Kumo does not bind to piRNA cluster at *42 AB*. qPCR after chromatin immunoprecipitation with Myc-Kumo and IgG control at piRNA locus cluster *42AB*. Percent input immunoprecipitated is shown for each primer set. Error bars indicate standard deviation from two independent experiments.

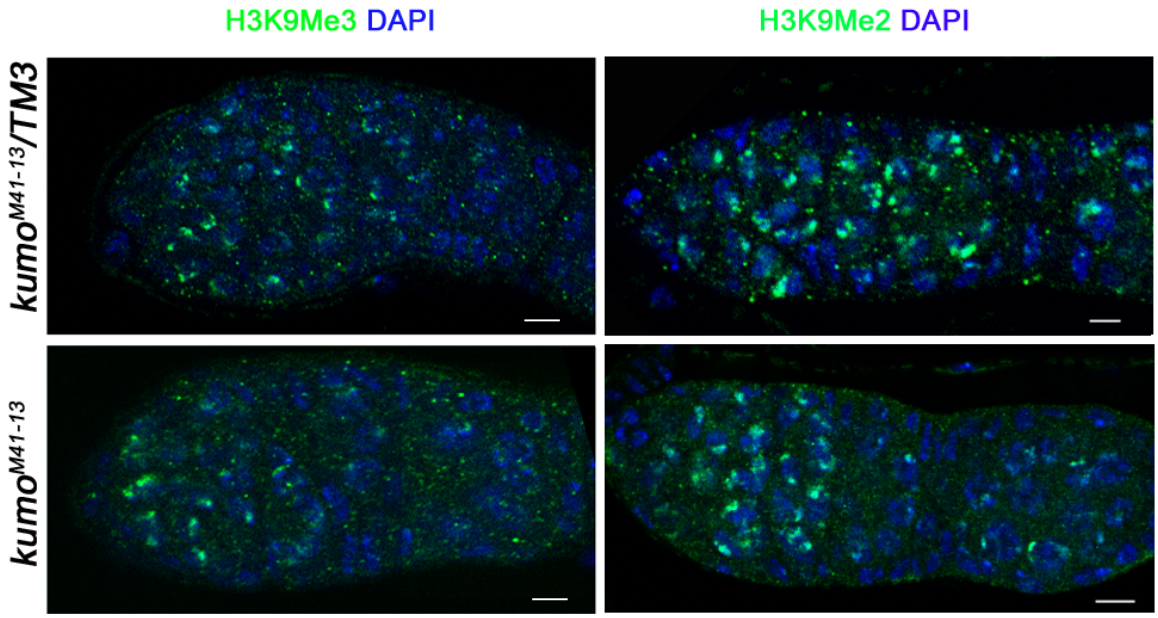

Figure S15. *kumo* mutants do not show a significant change in the localization patters of silencing marks H3K9Me3 and H3K9Me2. Immunostaining for H3K9Me3 and H3K9Me2 (both in green) do not show a significant variation in their respective expression patters between *kumo* heterozygous and mutant germaria. Nuclei were stained by DAPI (blue). Scale bars: 5µm

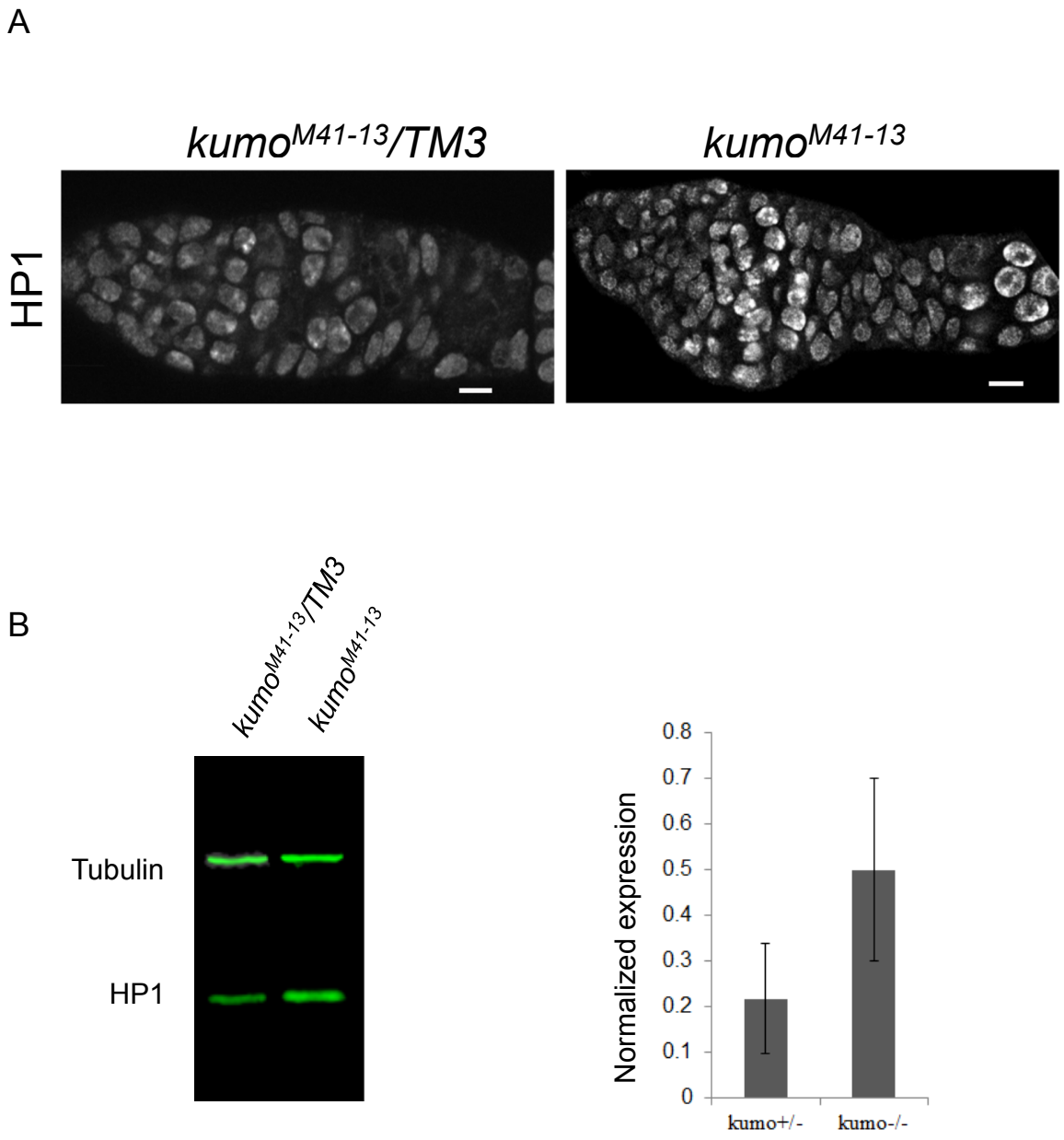

a

Figure S16. High expression of HP1 in *kumo* mutant germarium and early stage egg chambers. (A) Immunostaining for HP1 shows high HP1 expression in the *kumo* mutants germarium. Scale bars-5µm. (B) Quantitative Western analysis to compare HP1 expression between heterozygous control and the *kumo* mutants using lysates prepared from germaria and early stage egg chambers (up to stages 4 to 6). Quantification on the right indicates around 2.2 fold high expression of HP1 in the *kumo* mutant (n=3).